PHILOSOPHICAL TRANSACTIONS B

royalsocietypublishing.org/journal/rstb

Research

Cite this article: Richter AS, Tohge T, Fernie AR, Grimm B. 2020 The *genomes uncoupled*-dependent signalling pathway coordinates plastid biogenesis with the synthesis of anthocyanins. *Phil. Trans. R. Soc. B* **375**: 20190403.
http://dx.doi.org/10.1098/rstb.2019.0403

Accepted: 2 August 2019

One contribution of 20 to a theme issue 'Retrograde signalling from endosymbiotic organelles'.

Subject Areas:
plant science, cellular biology

Keywords:
retrograde communication, genomes uncoupled, anthocyanin, flavonoid

Author for correspondence:
Andreas S. Richter
e-mail: andreas.richter@hu-berlin.de

†Present address: Graduate School of Science and Technology, Nara Institute of Science and Technology, Ikoma, Nara, 630-0192, Japan.

Electronic supplementary material is available online at https://doi.org/10.6084/m9.figshare.c.4934778.

THE ROYAL SOCIETY PUBLISHING

The *genomes uncoupled*-dependent signalling pathway coordinates plastid biogenesis with the synthesis of anthocyanins

Andreas S. Richter[1,2], Takayuki Tohge[3,†], Alisdair R. Fernie[3] and Bernhard Grimm[1]

[1]Plant Physiology, and [2]Physiology of Plant Cell Organelles, Institute of Biology, Humboldt-Universität zu Berlin, Philippstrasse 13, 10115 Berlin, Germany
[3]Max-Planck-Institute of Molecular Plant Physiology, Am Mühlenberg 1, 14476 Potsdam-Golm, Germany

ASR, 0000-0002-2293-7297

In recent years, it has become evident that plants perceive, integrate and communicate abiotic stress signals through chloroplasts. During the process of acclimation plastid-derived, retrograde signals control nuclear gene expression in response to developmental and environmental cues leading to complex genetic and metabolic reprogramming to preserve cellular homeostasis under challenging environmental conditions. Upon stress-induced dysfunction of chloroplasts, GENOMES UNCOUPLED (GUN) proteins participate in the repression of *PHOTOSYNTHESIS-ASSOCIATED NUCLEAR GENES* (*PHANGs*). Here, we show that the retrograde signal emitted by, or communicated through, GUN-proteins is also essential to induce the accumulation of photoprotective anthocyanin pigments when chloroplast development is attenuated. Comparative whole transcriptome sequencing and genetic analysis reveal GUN1 and GUN5-dependent signals as a source for the regulation of genes involved in anthocyanin biosynthesis. The signal transduction cascade includes well-known transcription factors for the control of anthocyanin biosynthesis, which are deregulated in *gun* mutants. We propose that regulation of *PHANGs* and genes contributing to anthocyanin biosynthesis are two, albeit oppositely, co-regulated processes during plastid biogenesis.

This article is part of the theme issue 'Retrograde signalling from endosymbiotic organelles'.

1. Background

Owing to their sessile lifestyle, plants had to evolve strategies to cope instantaneously with biotic and abiotic stress such as pathogens, changing light intensities, temperature and nutrient availability. On a molecular level, the stress response includes a complex genetic and metabolic reprogramming to preserve cellular homeostasis and to allow growth under challenging conditions. The processes of acclimation to a changing environment are active from the beginning of germination through adolescence. In recent years, it became evident that abiotic stress is perceived, integrated and communicated through chloroplasts, the energy facility of photoautotrophic organisms. Stress responses which are initiated by chloroplast-derived signals feed so-called retrograde signalling pathways that aim at regulating the expression of nucleus-encoded genes. Although they cannot always be strictly separated, retrograde signals can be distinguished between those important during early developmental stages when the proplastid-to-chloroplast transition occurs (biogenic control) and signals from fully developed chloroplasts which are part of the so-called 'operational control' [1]. The latter group of signals, encompasses metabolites of biochemical pathways such as the isoprenoid biosynthesis [2–4], nucleotide metabolism [5,6], tetrapyrroles [7,8], the redox-status of plastid components [9–11] as well as reactive

oxygen species (ROS) emerging from photosynthesis [12–16], intermediates, end and breakdown products of carotenoid biosynthesis [17,18] and fatty acids (derivatives). Plastid gene expression also contributes to the regulation of nuclear-encoded genes [11,19–22]. The retrograde signalling pathways preserve cellular homeostasis mainly through transcriptional and post-transcriptional regulation of (stress) specific genes in the nucleus [23–26] but also through, for example, degradation of ROS-damaged plastids [27] or adjustment of morphological traits [28]. One of the retrograde signalling pathways acting during plastid biogenesis depends on the plastid-localized GENOMES UNCOUPLED (GUN) proteins, but the identity of the precise signals and function of the contributing components and mechanisms are still limited. In the course of plastid development, nucleus-encoded *PHOTOSYNTHESIS-ASSOCIATED NUCLEAR GENES* (*PHANGs*), such as genes encoding components of the photosynthetic electron transfer chain (*LIGHT HARVESTING COMPLEX* (*LHCs*) or *PLASTOCYANIN* (*PC*)), are highly expressed. When plastid biogenesis is disturbed, *PHANGs* are repressed [29–31]. GUN1, a plastid-localized pentatricopeptide repeat protein identified as one component in the retrograde communication pathway to regulate *PHANG* expression, was isolated almost three decades ago [30]. Extensive genetic and biochemical analysis revealed contributions of GUN1 to various aspects of plastid physiology and biochemistry such as plastid gene expression, RNA editing, proteostasis and protein import [32–42]. In addition to GUN1, genetic perturbation of Mg-chelatase (MgCh), a key enzyme of plastid-localized chlorophyll biosynthesis, leads to uncoupling of *PHANG* expression from the developmental state of plastids. Mutants of GUN4 (a positive regulator of MgCh), GUN5 (the catalytic subunit of MgCh) [43,44] and, although to a lesser extend compared to *gun5*, also of the I and D subunit of MgCh show a *gun* phenotype, i.e. reduced repression of *PHANGs* when chloroplast development is perturbed in *Arabidopsis* and barley [45,46]. Alteration of haeme metabolism in *gun2* (*HEME OXYGENASE*), *gun3* (*PHYTOCHROMOBILLIN SYNTHASE*), *gun6* (*FERROCHELATASE I* overexpressor line) and potentially also in *gun4* and *gun5* placed haeme, rather than other tetrapyrrolic intermediates [47,48], in the centre of current models for retrograde signal(s) emerging from tetrapyrrole biosynthesis [7,37,49]. In addition, CRYPTOCHROME 1 (CRY1) and downstream signalling components such as ELONGATED HYPOCOTYL 5 (HY5) [31] or GOLDEN2-LIKE 1 and 2 [50–52] play an important role for the retrograde control of nuclear gene expression.

One of the major traits of plants suffering from adverse environmental conditions, like high light or temperature shifts, is the accumulation of coloured anthocyanin pigments in above-ground tissues. Although dispensable for growth under optimal conditions, these secondary metabolites were shown to protect plants from excessive amounts of light [53–55]. Anthocyanins are end products of a combined pathway of cytosolic phenylpropanoid and flavonoid biosynthesis, which produces a great diversity of polyphenolic plant secondary metabolites [56]. After the conversion of plastid-derived phenylalanine to *p*-coumaroyl CoA through PHENYLALANINE AMMONIA LYASE (PAL), CINNAMIC ACID-4-HYDROXYLASE (C4H) and 4-COUMAROYL COA LIGASE (4CL), CHALCONE SYNTHASE (CHS) catalyses the initial step of flavonoid biosynthesis (figure 1*a*). Subsequent reactions provide the precursor(s) for various flavonoid derivatives [57]. The main route for the synthesis of anthocyanins branching from core flavonoid/anthocyanin biosynthesis (FAB) is initiated by DIHYDROFLAVONOL 4-REDUCTASE (DFR) and LEUCOANTHOCYANIDIN DIOXYGENASE (LDOX) [58–60]. The FAB pathway is divided into two major parts which consist of enzymes encoded by 'early biosynthetic genes' (*EBGs*), like *CHS*, and the 'late biosynthetic genes' (*LBGs*), such as *DFR* and *LDOX*. Diminished pathway activity in *FAB* mutants often coincides with the lack of oxidized tannins in the seed coat and a *transparent testa* (*tt*) (seed coat) phenotype [58]. In leaves, enzymes and regulators of FAB are targets for post-translational protein modifications [61–63]. *EBGs* are controlled by a set of partially redundant transcription factors (TF) MYB11, MYB12 and MYB111 [64,65]. By contrast, *LBG* transcription is mainly regulated by an MBW-complex consisting of MYB, bHLH and WD40 TF. Together with one WD40 variant (*TRANSPARENT TESTA GLABRA 1*), *MYB75* encoding PRODUCTION OF ANTHOCYANIN PIGMENT 1 (PAP1) and the bHLH TFs TT8, *GLABRA3* (GL3) and *ENHANCER GL3* (EGL3) these major factors concertedly regulate the composition and activity of the MBW-complex [66–68]. The exchange of PAP1 by MYBL2 inactivates the complex [69–72]. *EBGs*, *LBGs* and TFs have been shown to be under the control of light signalling pathways involving ultraviolet-, blue and red-light photoreceptors and the downstream component HY5 [73–77]. The role of chloroplast-derived signals (including phytohormones and ROS) and their downstream components on the regulation of the cytosolic FAB pathway have been previously discussed [16,55,78–80]. However, the identity of signal molecules and the underlying mechanisms by which, in particular, plastid biogenesis contributes to the regulation of FAB are still scarce.

2. Results

(a) Induction of anthocyanin biosynthesis upon block of chloroplast development

Norflurazon (NF) is an inhibitor of plastid-localized carotenoid biosynthesis which is routinely applied to germinating seedlings to suppress chloroplast development from undifferentiated pro-plastids [30,81]. When germinated in the presence of NF, plant leaves lack carotenoids and do not accumulate chlorophyll and chlorophyll-binding proteins resulting in the development of white cotyledons (figure 1*b*). Also, and in contrast to control plants grown without NF, light-grown, NF-treated *Arabidopsis thaliana* wild-type plants (WT, Col-0) showed a purple coloration, which was attributable to the accumulation of anthocyanins (figure 1*b*,*c*). While etiolated plants showed the same basal level of anthocyanins in the presence and absence of NF, anthocyanin accumulation was stimulated by three to fourfold in light, when chloroplast development was perturbed (figure 1*c*). At the same time, two light-inducible representative *PHANGs* (*CA1* and *LHCB1.2*), were repressed in the light, but not in the dark-grown NF-treated plants (figure 1*d*,*e*). Visible accumulation of anthocyanins in the NF-treated tissues resulted from strong induction of *EBG* and *LBG* expression. In contrast to the untreated control, transcripts coding for *CHS*, *CHI*, *DFR* and *LDOX* were enriched by 5–10-fold when plants germinated in the presence of NF (figure 1*f*–*i*). Higher expression of *FAB* was explained by induction of three major TFs (*MYB12*, *MYB75* (PAP1) and *HY5*) as well as a reduced transcription of the *MYBL2* repressor in the light (figure 1*j*–*m*).

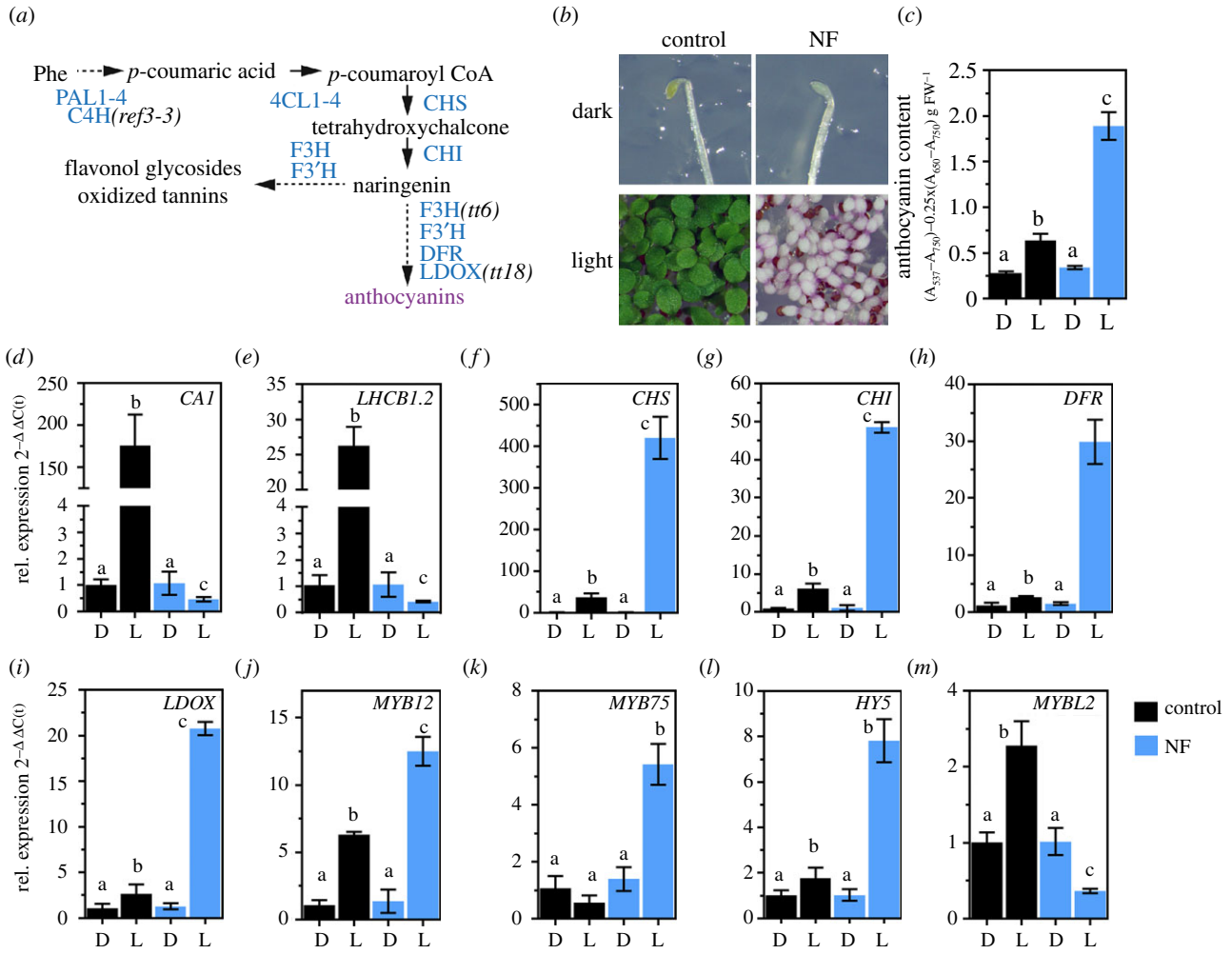

Figure 1. Induction of flavonoid/anthocyanin biosynthesis (FAB) upon chloroplast dysfunction. (*a*) Schematic overview of the FAB pathway leading to the formation of polyphenolic compounds. PAL1-4, PHENYLALANINE AMMONIA LYASE; C4H, CINNAMIC ACID 4-HYDROXYLASE; 4CL1-4, 4-COUMAROYL COA LIGASE 1-4; CHS, CHALCONE SYNTHASE; CHI, CHALCONE ISOMERASE; F3H, FLAVANONE 3-HYDROXYLASE; F3'H, FLAVONOID 3'-HYDROXYLASE; DFR, DIHYDROFLAVONOL-4-REDUCTASE; LDOX, LEUCOANTHOCYANIDIN DIOXYGENASE. (*b*) Representative photograph of etiolated (dark) and continuous light-grown *Arabidopsis thaliana* Col-0 seedlings germinated in the absence (control) or presence of norflurazon (NF). (*c*) Quantification of anthocyanins in seedlings shown in (*b*). Data are given as mean ± s.d. ($n = 4$). Letters indicate statistical groups determined by Student's *t*-test ($p < 0.05$). FW, fresh weight. Black (control) and blue (NF). (*d–m*) qRT-PCR analysis of gene expression for genes encoding *PHANGs* (*CARBONIC ANHYDRASE1* and *LIGHT HARVESTING COMPLEX B1.2*), enzymes involved in FAB and transcription factors (*MYB12*, *MYB75*, *HY5*, *MYBL2*). Seedlings were grown as described in (*b*). D, dark; L, light. Gene expression was calculated relative to the WT etiolated in the absence of NF and *ACTIN2* as reference (ΔΔC(t)method). Data are given as mean ± s.d. ($n = 4$). Letters indicate statistical groups determined by Student's *t*-test ($p < 0.05$).

(b) Involvement of the GUN-dependent signalling pathway

Because *PHANGs* were shown to be under GUN-dependent retrograde control when chloroplast development is altered, we tested if the same plastid-to-nucleus communication is responsible for the induction of anthocyanin biosynthesis. For this purpose, previously published leaky *gun1-1* (electronic supplementary material, figure S4), *gun4-1*, *gun4-3* and *gun5-1* were compared with NF-treated WT plants, other mutants of the tetrapyrrole biosynthesis pathway (e.g. *chlm* (encoding MgP methyltransferase), *ch1-2* (chlorophyll *a* oxygenase)) and for components of the thylakoid protein integration pathway (cp*srp43/54*, see the electronic supplementary material, table SII). After growth on NF, cotyledons of all genotypes—except the four *gun* mutants—showed a strong purple coloration (figure 2*a*). The *gun* mutants defective in retrograde signalling, on the other hand, showed less purple coloration and accumulated only 40–70% of the anthocyanin content detected in the WT (figure 2*d*). Metabolic profiling confirmed the reduced accumulation of the major anthocyanins but not of the flavonoid/anthocyanin precursor phenylalanine in *gun1*, *gun4* and *gun5* mutants germinated in the presence of NF (electronic supplementary material, figure S1). As expected, the expression of two representative *PHANGs* (*CA1* and *LHCB1.2*) was repressed to the WT level in *chlm*, *ch1-2* and *srp43/54*, but were less downregulated in *gun1-1*, *gun4-1*, *gun4-3* and *gun5-1* mutants (figure 2*a*,*b*). We also examined the role of GUN-dependent signalling during acclimation to environmental stress and treated soil-grown WT, *gun* and non-*gun* mutant genotypes with high light (HL) for a period of 24 h and determined anthocyanin and chlorophyll (Chl) content (electronic supplementary material, figure S2). While the *gun1-1* mutant showed WT-like Chl content, mutant genotypes affected in Chl synthesis (*gun4*, *gun5*, *chl27* (MgPMME oxidative cyclase), *ch1- 2*) accumulated 50–70% of the Chl amounts detected in the WT plants at the beginning of the HL shift (electronic supplementary material, figure S2A). During the 24 h of HL treatment, the Chl content decreased by approximately 30% in the WT, and a similar trend was observed for the mutants. HL exposure induced WT-like accumulation of anthocyanins in *gun1-1* mutant plants with a gradual increase of

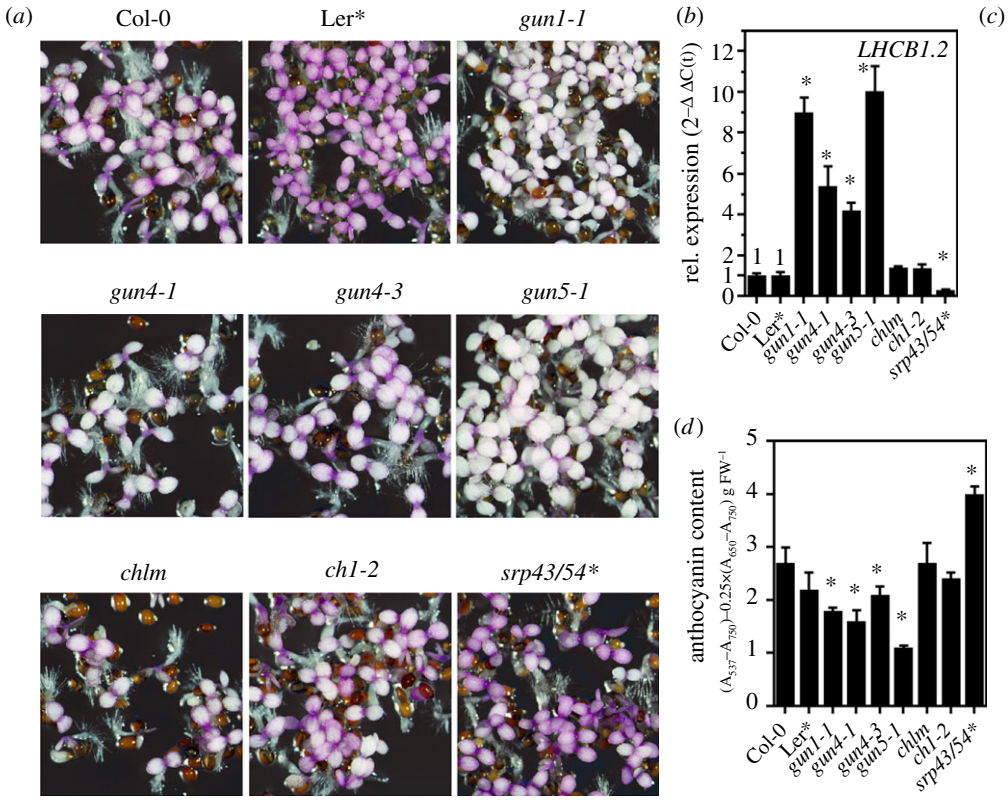

Figure 2. Induction of FAB depends on *genomes uncoupled* retrograde signalling. (*a*) Representative photograph of 5-day-old *Arabidopsis thaliana* genotypes grown in continuous light in the presence of norflurazon. For the double mutant of cpsrp43/54, the *Landsberg erecta* ecotype was used as control (*). (*b*,*c*) qRT-PCR analysis of gene expression for genes encoding *PHANGs* (*CARBONIC ANHYDRASE1* and *LIGHT HARVESTING COMPLEX B1.2*). Gene expression was calculated relative to the NF-treated WT as control and *ACTIN2* as reference (ΔΔC(t)method). Data are given as mean ± s.d. ($n = 3$). Asterisks indicate statistical significance relative to the WT controls determined by Student's *t*-test ($p < 0.05$). (*d*) Quantification of anthocyanins in seedlings shown in (*a*). Data are given as mean ± s.d. ($n = 3$). Asterisks indicate statistical significance relative to the WT controls determined by Student's *t*-test ($p < 0.05$). FW, fresh weight.

anthocyanin pigment content (electronic supplementary material, figure S2B). By contrast, *gun4-1*, *gun4-3*, *gun5-1* as well as the non-*gun* genotypes (*chl27*, *ch1-2*) showed diminished accumulation of anthocyanins during and at the end, respectively, of the HL treatment (electronic supplementary material, figure S2B). This finding indicates that de-regulation of FAB is a *gun* specific property during early plastid biogenesis only.

To analyse the anthocyanin deficiency in *gun* mutants after NF treatment further, we analysed global transcriptome profiles of NF-treated WT, *gun1-1*, *gun4-1* and *gun5-1* using RNA-sequencing. Heat map representation of the approximately 9300 significantly deregulated genes (SDGs) in at least one of the *gun* mutants ($0 < \log2$ fold change > 0, adjusted *p*-value 0.05, electronic supplementary material, table SI) revealed a strikingly similar transcriptome response of the NF-treated *gun* mutants compared to the NF-treated WT (figure 3*a*). Because *gun4-1* showed only a weak *gun* phenotype in comparison to, for example, *gun5* (figure 2*b*,*c*) the overlap of SDG between *gun1* and *gun5* was always bigger than the overlap of *gun4-1* with the other genotypes (figure 3*b*,*c*). Out of the 5056 upregulated transcripts, 690 were significantly deregulated in all *gun* mutants (figure 3*b*). Within this cluster, *PHANGs* were identified (electronic supplementary material, table SI). By contrast, the cluster of commonly downregulated transcripts (443 in all *gun*, figure 3*c*) included genes of the phenylpropanoid/FAB explaining the anthocyanin deficiency of the *gun* mutants. We, therefore, analysed both, the upregulated and downregulated clusters for transcripts whose gene products are involved in or related to FAB. Because *gun1-1* and *gun5-1* showed an almost similar transcriptome response, we focused on *gun1-1* and *gun5-1* in further experiments. Expression of mRNAs coding for enzymes involved in anthocyanin biosynthesis (*PAL4*, *4CL2*,*3*,*5*, *TT4*, *TT5*, *F3H*, *DFR* and *LDOX*) as well as transcripts of major TFs such as *MYB11*, *MYB111*, *MYB75* were found to be downregulated with the same tendency in *gun1-1* and *gun5-1* (figure 3*d*). On the other hand, *4CL1*, *PAL2* and the transcriptional repressor *MYBL2* were stronger expressed in *gun1-1* and *gun5-1* compared to the NF-treated WT, while the bHLH TF TT8 was repressed in *gun5-1*, but induced in *gun1-1* (figure 3*d*). We confirmed the differential expression of transcripts identified by RNAseq with quantitative real-time polymerase chain reaction (qRT-PCR) analysis using cDNA obtained from independently grown seedlings and compared the expression of the *FAB* genes in NF-treated *gun* relative to NF-treated WT (figure 3*e*,*f*). A strong positive correlation between expression values of RNAseq and qRT-PCR confirmed the de-regulation of *FAB* gene expression in *gun* mutants when plastid development is suppressed. However, it is important to mention that the expression of *LBGs* (*DFR*, *LDOX*) was always stronger affected than *EBGs* (*CHS*, *CHI*).

(c) Anthocyanins do not control *PHANG* expression

The strong negative correlation between *PHANG* and *FAB* expression, i.e. *gun* phenotype and anthocyanin accumulation, prompted us to hypothesize that anthocyanins might be involved in the GUN-dependent signalling pathway responsible for the repression of *PHANGs*. Therefore, a mutant of the early steps of the phenylpropanoid biosynthesis preceding FAB was analysed. As expected, the *ref3-3* mutant, expressing

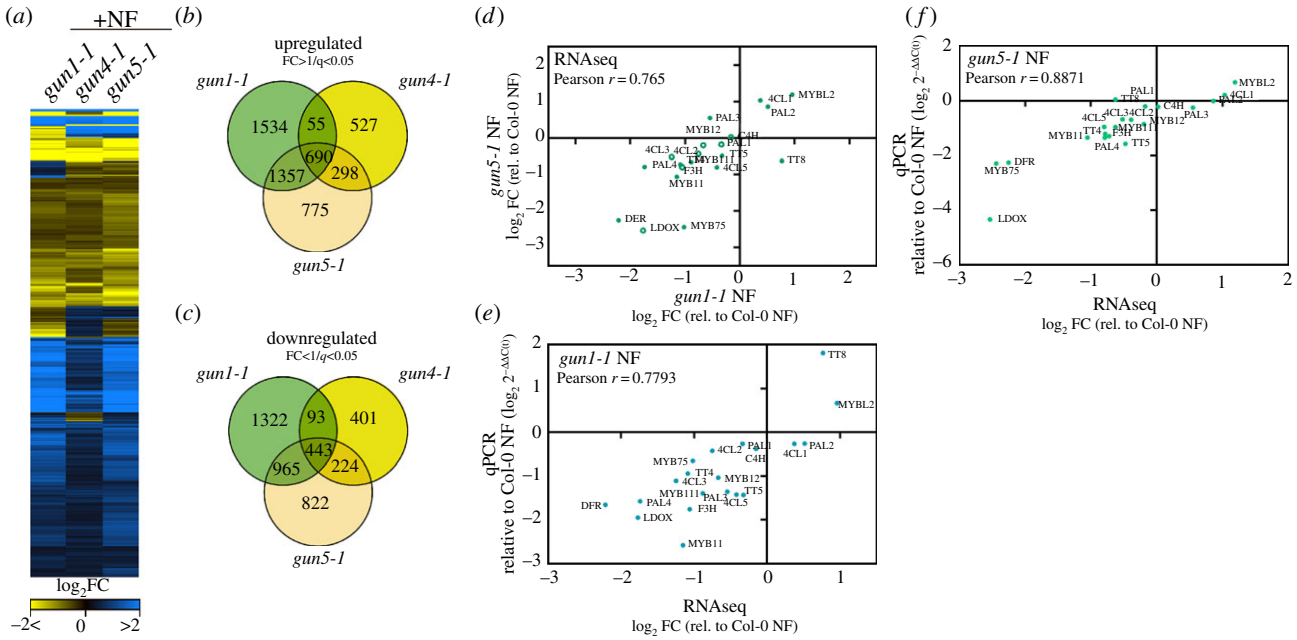

Figure 3. RNA-seq analysis of transcript changes in norflurazon (NF)-treated WT Col-0, *gun1-1*, *gun4-1* and *gun5-1* mutants. (*a*) Heat map representation of significantly deregulated genes (SDGs) for each genotype relative to the WT control ($q < 0.05$, $0 < \log2(\text{fold change}) > 0$). The RNA-seq experiment was performed, and the results analysed as described in the Materials and methods section. (*b,c*) Venn diagrams representing the degree of overlap between upregulated (B, fold change > 1) and downregulated (C, fold change < 1) SDGs in the *gun* mutants. SDGs relative to the WT control were selected based on $q < 0.05$ (p-value adjusted for the false discovery rate). (*d*) Comparison of *FAB* transcript abundance in the *gun1-1* and *gun5-1* transcriptome datasets. Closed circles denote statistical significance relative to the NF-treated WT ($q < 0.05$). Abbreviations for genes are explained in figure 1 and in the main text. (*f,e*) Confirmation of the RNA-seq result by qRT-PCR analysis. Expression of selected transcripts was analysed with cDNA obtained from independent growth of seedlings and was compared to the expression values obtained from the RNA-seq experiments. Gene expression in NF-treated *gun* mutants was calculated relative to the NF-treated WT and *ACTIN2* as reference (ΔΔC(t)method). (*d,e*) Pearson $r > 0.75$ indicates a positive correlation between the different datasets and analysis.

a point-mutated *C4H* gene (figure 1*a*; electronic supplementary material, figure S3A/B), showed reduced accumulation of anthocyanins compared to WT when germinated in the presence of NF (figure 4*a*). Although anthocyanin accumulation was even more impaired in *ref3-3* compared to *gun1*, *PHANG* expression was suppressed to WT levels after NF treatment (figure 4*b,c*), indicating that anthocyanin levels do not determine the transcription rate of *PHANGs*. This finding was further supported by the fact that diminished anthocyanin accumulation in *ref3-3 gun1-1* and *ref3-3 gun5-1* compared to the single mutants did not lead to enhanced *PHANG* expression (figure 4*a–c*). Likewise, knockout of the genes encoding the FAB enzymes flavanone 3-hydroxylase (F3H), and LDOX designated *tt6* and *tt18*, respectively (electronic supplementary material, figure S3C/D) prevented the accumulation of anthocyanins after NF treatment but not the repression of *LHCB1.2* (figure 4*d,e*). Additionally, overexpression (*pap1-D*) and knockout of *MYB75* (*myb75*) positively and negatively affected anthocyanin biosynthesis upon NF treatment, respectively, but did not trigger a *gun* phenotype (figure 4*d–f*). The lack of a *gun* phenotype of mutants defective in FAB is in agreement with *gun* mutant screens which yielded no FAB mutant. In summary, anthocyanins are excluded to control *PHANG* expression, but the results reveal *FAB* genes as an additional target of the GUN-dependent retrograde signalling pathway when chloroplast development is perturbed.

(d) Activation of anthocyanin biosynthesis depends on GUN1 and GUN5

To obtain detailed insights on how the GUN1 and GUN5 specific signals influence FAB, we compared light-exposed *gun1-1*, *gun5-1*, and *gun1-1 gun5-1* with the WT in the absence or presence of NF (figure 5). While *gun1-1* showed WT-like anthocyanin levels in the control condition without NF, *gun5-1* accumulated less anthocyanins, and anthocyanin deficiency was even more pronounced in *gun1-1 gun5-1* plants (figure 5*a,b*). Stimulated expression of *FAB* genes (figure 1) led to 2-3-fold higher anthocyanin content in the treated WT compared to the control without NF. By contrast, NF-treated *gun1-1* and *gun5-1* accumulated only 60% and 30%, respectively, of the WT anthocyanin content. To test if knock out of *GUN1* exacerbates anthocyanin deficiency in comparison to leaky *gun1-1* mutant and *gun5-1*, we additionally analysed a loss-of-function allele of *GUN1* (*gun1-102*, [38]). While knock out of *GUN1* enhanced uncoupling of *PHANG* expression (electronic supplementary material, figure S4C), the phenotype (electronic supplementary material, figure S4A) and anthocyanin content (electronic supplementary material, figure S4B) of *gun1-102* was indistinguishable from that of *gun1-1* after NF-treatment. In agreement, expression of *FAB* pathway genes was reduced to the same extent in both *GUN1* alleles (electronic supplementary material, figure S4D). Stimulation of FAB was hardly detectable in NF-treated *gun1-1 gun5-1* compared to the control condition, and anthocyanin level did not even reach the level of the untreated WT (figure 5*b*). In stark contrast to induced *FAB* genes in the NF-treated WT (figure 1 and figure 5*c*), NF-treated *gun* mutants showed diminished induction of *FAB* genes compared to the control condition (figure 5*c*). Furthermore, an additive effect of GUN1 and GUN5 mutation was found in *gun1-1 gun5-1* relative to the single mutants on the expression, for example, of *MYB75* and *DFR* (figure 5*c*). Consequently, *gun1-1 gun5-1* accumulated fewer anthocyanin pigments than the single mutants (figure 5*b*).

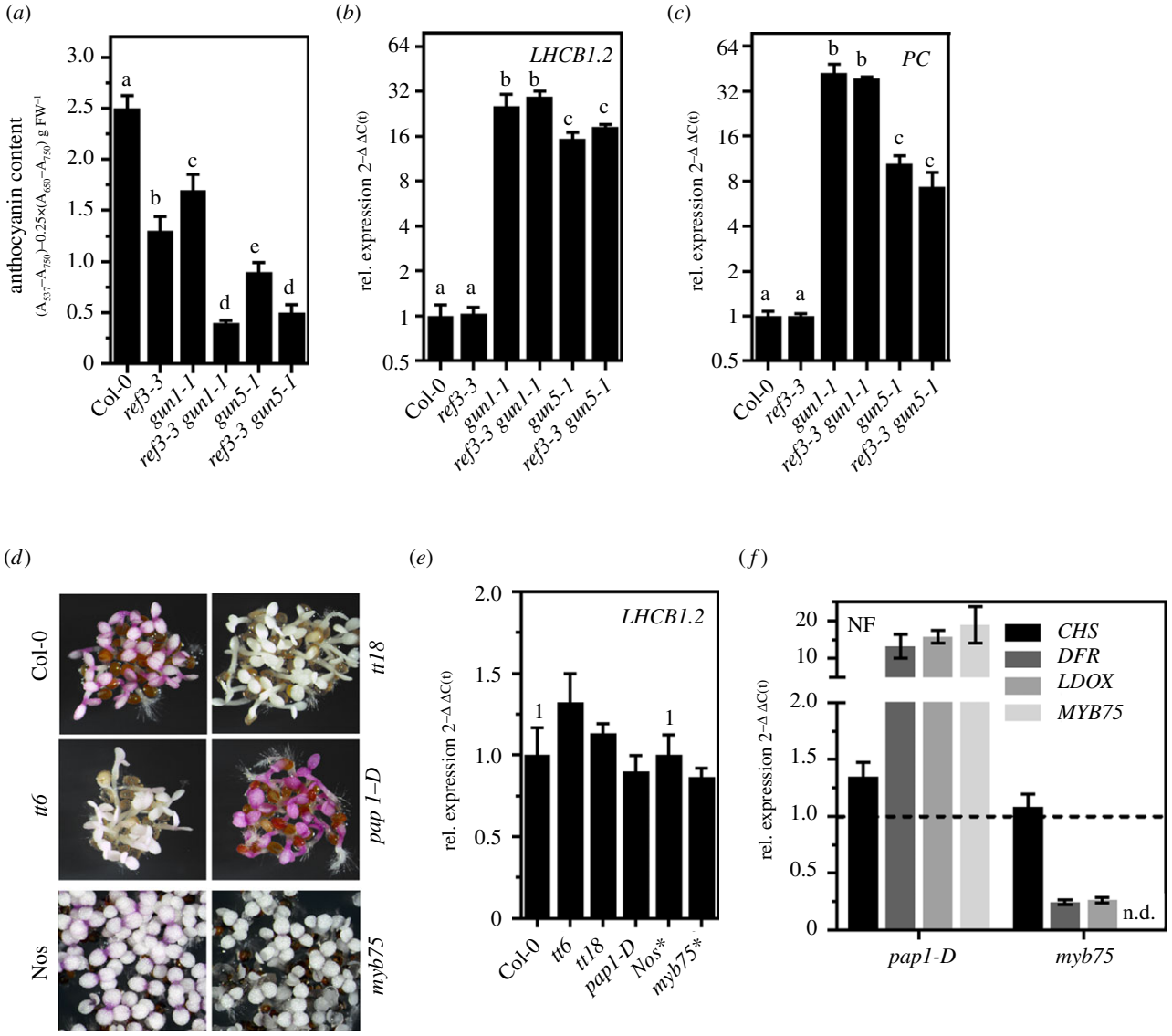

Figure 4. Anthocyanins do not control *PHANG* expression. (*a*) Quantification of anthocyanins in seedlings grown for 5 d in continuous light in the presence of NF. WT, *gun1-1*, *gun5-1*, *ref3-3* (point mutant for *C4H*) and double mutants were analysed. Data are given as mean ± s.d. ($n = 4$). Letters indicate statistical groups determined by Student's *t*-test ($p < 0.05$). FW, fresh weight. (*b,c*) qRT-PCR analysis of gene expression for genes encoding *PHANGs* (*CARBONIC ANHYDRASE1* and *PLASTOCYANIN*). Data are given as mean ± s.d. ($n = 3$). Letters indicate statistical groups determined by Student's *t*-test ($p < 0.05$). (*d*) Representative photograph of 5 d-old WT (Col-0 and Nos), *transparent testa (tt) 6*, *tt18*, the dominant *pap1-D* overexpression line and *myb75* mutant grown in continuous light in the presence of norflurazon. (*e*) qRT-PCR analysis of gene expression for *LIGHT HARVESTING COMPLEX B1.2* in genotypes shown in (*d*). (*f*) qRT-PCR analysis of *CHS*, *DFR*, *LDOX* and *MYB75* expression in *pap1-D* and *myb75* mutant grown in the presence of NF. For the analysis shown in (*b,c,e,f*) the expression was calculated relative to the NF-treated WT and *ACTIN2* as reference (ΔΔC(t)method). Data are given as mean ± s.d. ($n = 3$). The *Nossen* ecotype was used as control for the myb75 mutant (*).

The blue light photoreceptor CRY1 and the downstream acting TF HY5 are essential for light induction of *FAB*. As reported previously, *cry1-2* and *hy5* mutants showed a modified expression of *CHS* and *LDOX* and, consequently, reduced anthocyanin content compared to WT seedlings when treated with NF (figure 5*d*,*e*). Reduced *FAB* gene expression was more pronounced in *cry1-2* seedlings and resembled the *FAB* transcript level of NF-treated *gun* mutants. In summary, the results suggest that *FAB* genes were downregulated by two independent GUN signals and proper activation of FAB depended on a concerted action of both plastid signals and light signalling pathways.

(e) Evidence for a function of MYBL2

Regulation of gene expression for FAB is mediated through the activity of the MBW-complex, which includes the essential MYB component, such as *MYB75* (PAP1). When MYBL2 replaces PAP1, the activity of the MBW-complex is diminished. In the presence of NF, an *MYBL2* knockout line (*mybl2-2*) accumulated more anthocyanins compared to the WT (figure 6*a*), which was explained by transcriptional induction of *MYB75* (figure 6*c*), *DFR* and *LDOX* (figure 6*d*). This result confirmed the important function of MYBL2 in counteracting *FAB* gene expression and anthocyanin biosynthesis, respectively, in NF-treated *Arabidopsis* seedlings [69,71]. Interestingly, *MYBL2* was expressed to a higher level in the *gun* mutants compared to WT (figures 3 and 6*c*). We, therefore, analysed crosses of *mybl2-2* with either *gun1-1* or *gun5-1* for the potential impact of MYBL2 on the downregulated *FAB* expression (figure 6*c*). MYBL2 deficiency did not interfere with the *gun* phenotype observed in the single mutants (figure 6*b*). Surprisingly, and in stark contrast to *mybl2-2*, *MYB75* transcript levels did not differ between *gun* single and *mybl2-2 gun1-1* or

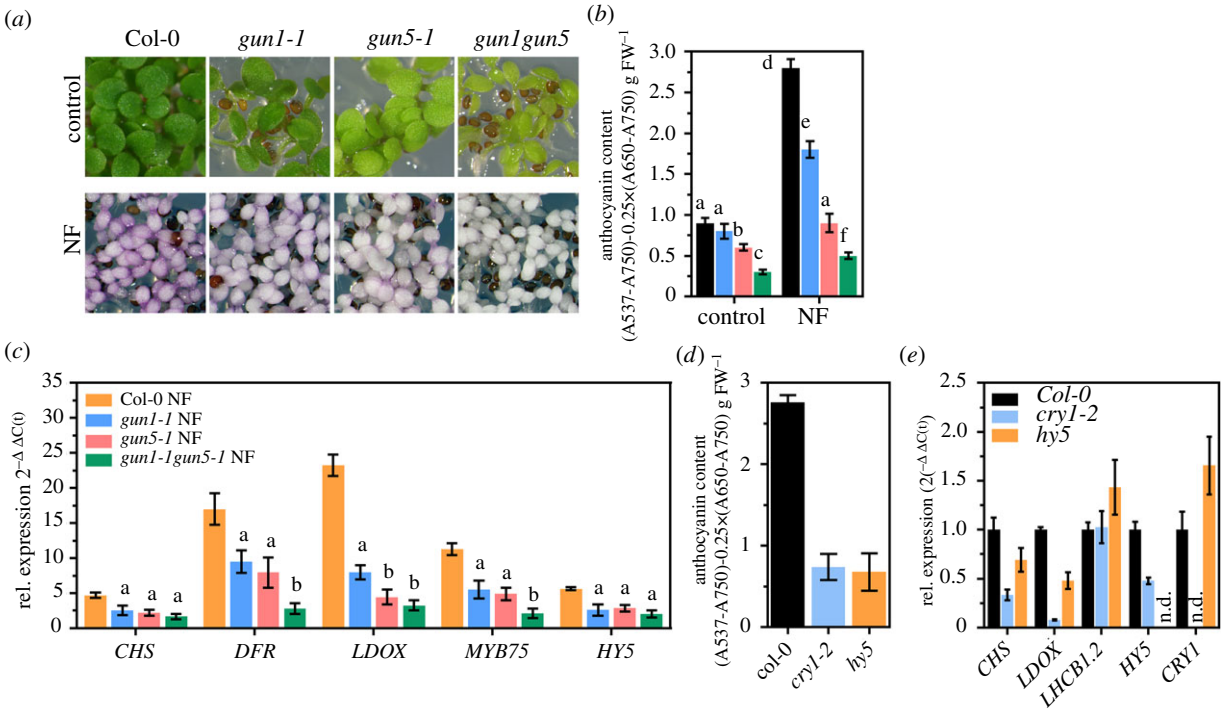

Figure 5. Induction of FAB involves GUN1, GUN5, and components of light signalling. (*a*) Representative photograph of 5 d-old Col-0, *gun1-1*, *gun5-1* and *gun1-1 gun5-1* double mutant grown in continuous light in the absence (control) or presence of norflurazon (NF). (*b*) Quantification of anthocyanins in the seedlings shown in (*a*). Data are given as mean ± s.d. ($n = 4$). Letters indicate statistical groups determined by Student's *t*-test ($p < 0.05$). FW, fresh weight. (*c*) qRT-PCR analysis of gene expression for gene products involved in FAB and transcription factors. Gene expression was calculated relative to the control without NF for each genotype and *ACTIN2* as reference (ΔΔC(t)method). Data are given as mean ± s.d. ($n = 4$). Letters indicate statistical significance relative to the NF-treated WT determined by Student's *t*-test ($p < 0.05$). (*d*) Quantification of anthocyanins in Col-0, *cry1-2* and *hy5* mutants grown in continuous light in the presence of NF. Data are given as mean ± s.d. ($n = 4$). FW, fresh weight. (*e*) qRT-PCR analysis of gene expression for genes encoding *CHS*, *LDOX*, *LHCB1.2*, *HY5* and *CRY1*. Gene expression was calculated relative to the NF-treated WT and *ACTIN2* as reference (ΔΔC(t)method). Data are given as mean ± s.d. ($n = 3$). n.d., not detectable.

mybl2-2 gun5-1 (figure 6*c*). *DFR* and *LDOX* expression were recovered to a *mybl2-2* level in *mybl2-2 gun1* but only to WT-like level in *mybl2-2 gun5-1* (figure 6*d*). As a result, stimulated expression of *FABs* in *mybl2 gun* double mutants gave rise to higher anthocyanin contents, which increased compared to the *gun* single mutants but were still lower compared to *mybl2-2* (figure 6*a*).

3. Discussion

(a) Plastid signals control flavonoid/anthocyanin biosynthesis

Stimulation of FAB and accumulation of end-products of the pathway, like anthocyanins, has been reported for plants suffering from nutrient starvation, changes in light quality and quantity as well as growth temperature (e.g. Kovinich, Kayanja [82]). Essential factors for the transcriptional and post-translational regulation of FAB, such as photoreceptors [75,76] and components of hormone signalling [72,80] have been described. Previous analysis also revealed a function of GUN1 in the regulation of FAB when chloroplast biogenesis is inhibited [16,36,41,83]. However, the knowledge about molecular mechanisms and factors of (*gun*-dependent) plastid signalling functioning in the regulation of FAB and, in particular, the importance of the tetrapyrrole-dependent signalling pathway is still incomplete. NF is commonly used to prevent the development of chloroplasts from proplastids. By blocking phytoene desaturase, NF diminishes the accumulation of carotenoids, which are essential factors for the stabilization, accumulation and function of the light-absorbing photosystems. When germinated in the presence of NF in the light, plants develop white cotyledons lacking functional chloroplasts (figure 1 and [30], Nott *et al.* [81]). As a result of the inhibition of plastid biogenesis, transcriptional induction of *FAB* pathway genes and strong accumulation of anthocyanins was observed (figure 1). Expression of genes encoding positive transcriptional regulators of *EBGs* (*MYB12*) and *LBGs* (*MYB75*) and of MYB75 itself (i.e. *HY5*, Shin *et al.* [74]) was induced upon NF treatment. By contrast, a negative regulator, *MYBL2*, which concurrently interacts with MYB75 (PAP1) for binding to the MBW-complex [71], was downregulated in NF-treated light-grown seedlings, allowing high expression of FAB pathway genes and anthocyanin accumulation. Diminished expression of *MYBL2* probably results from the stimulated expression of *HY5* [70,71,84]. Reduced accumulation of anthocyanins in *myb75* knockout mutants and elevated contents in a dominant *PAP1* (*MYB75*) overexpression line (figure 4), as well as over-accumulation of anthocyanins in a NF-treated knockout mutant line for the negative regulator MYBL2 (figure 6) also verified their function in regulating the composition and activity of the MBW-complex for the accumulation of anthocyanins when plastid development is suppressed. Stimulated mRNA transcription and activity of *CHS*, a key enzyme in the FAB pathway, was also observed in mustard seedlings treated with NF and the plastid specific translation inhibitor chloramphenicol, respectively [85]. Also, perturbed plastid development stimulated the strong accumulation of anthocyanins in young seedlings [41,83,86]. In summary, the

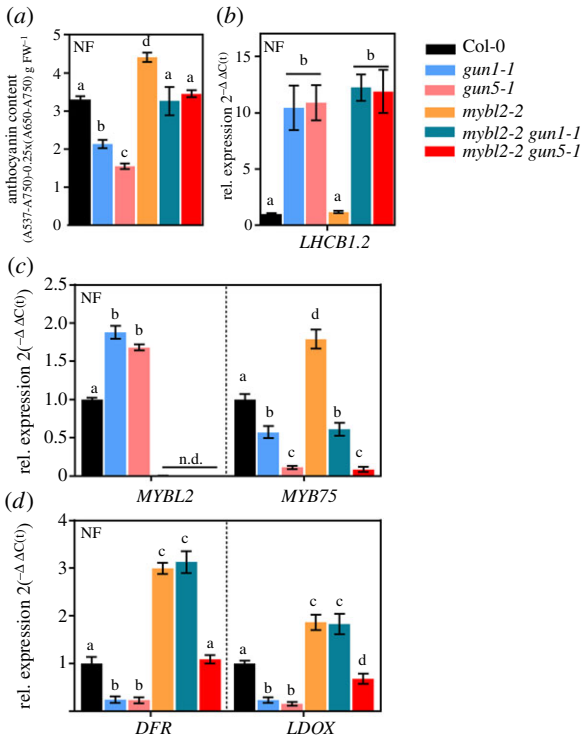

Figure 6. The impact of MYBL2 on FAB in *gun* mutants. (*a*) Quantification of anthocyanins in seedlings grown for 5d in continuous light in the presence of NF. WT, *gun1-1*, *gun5-1*, *mybl2-2* and double mutants of *gun* and *mybl2-2* were analysed. Data are given as mean ± SD ($n = 4$). Letters indicate statistical groups determined by Student's *t*-test ($p < 0.05$). FW, fresh weight. (*b–d*) qRT-PCR analysis of gene expression for *LHCB1.2* (*b*), *MYBL2 and MYB75* (*c*) and *DFR* and *LDOX* (*d*) in NF-treated seedlings. Gene expression was calculated relative to the NF-treated WT and *ACTIN2* as reference (ΔΔC(t)method). Data are given as mean ± s.d. ($n = 4$). Letters indicate statistical groups determined by Student's *t*-test ($p < 0.05$). n.d., not detectable.

results emphasize the important role of plastid-derived communication in regulating the expression and activity of the FAB pathway and synthesis of anthocyanins during plastid biogenesis.

(b) Regulation of flavonoid/anthocyanin biosynthesis by two GUN-dependent signals

Simultaneously to the induction of *FAB* genes, the block in chloroplast development led to suppressed *PHANG* expression in WT seedlings (figure 1). The repression of *PHANGs* is known to be mediated, at least partially, by the GUN-dependent retrograde signalling pathway and, consequently, *gun* mutants accumulated more *CA1* and *LHCB1.2* mRNAs upon perturbed plastid development (figure 2). At the same time, the modified function of GUN1, GUN4 and GUN5 prevented WT-like accumulation of anthocyanins (figure 2). Anthocyanin deficiency of *gun* mutants was found to be a result of modulated *FAB* gene expression (figures 3 and 5), rather than a shortfall in the supply of phenylalanine, the precursor of all phenylpropanoids and their derivatives (electronic supplementary material, figure S1). Even more important, although strongly induced in NF-treated WT seedlings, *FAB* genes were markedly less induced in *gun* mutants compared to the control without NF (figure 5). This result is indicative for either a negative signal emitted from *gun* plastids or a stimulating action of a *FAB* repressor (e.g. a TF) in *gun* mutants. Indeed, FAB is negatively affected by *MYBL2*, which interferes with the composition of the MBW TF complex [69,71]. MYBL2 was significantly upregulated in *gun1*, and *gun5* (figure 6) and knockout of *MYBL2* rescued the modified *LBG* expression of *gun1* but only partially that of *gun5*. These results indicated that MYBL2 contributes to GUN1-dependent control of *FAB* but plays a minor role in GUN5-mediated signalling. Hence, FAB/*FAB* regulation might also involve another dominant repressor (or the lack of an activator) in *gun5*.

The altered accumulation of anthocyanins in *gun1-1* seedlings observed here is in agreement with previous studies revealing anthocyanin deficiency of *gun1* mutants when plastid development is inhibited [36,41,83]. The recently demonstrated impairment of plastid protein import in *gun1* seedlings upon block of chloroplast biogenesis, helped, in addition to other studies, to distinguish GUN1-dependent from the tetrapyrrole biosynthesis-dependent signalling (i.e. GUN4/5) and verifies the synergistic effects of two independent signals emerging from GUN1 and tetrapyrrole biosynthesis, respectively [34,87]. In this context, double mutation of GUN1 and GUN5 exacerbated the anthocyanin deficiency of the single mutants (figure 5). Interestingly, the NF-treated *gun1 gun5* mutant accumulated similar amounts of anthocyanins as etiolated WT seedlings and the anthocyanin content did not even reach that of the light-grown WT in the absence of NF. Therefore, it could be assumed that, during the process of plastid biogenesis, regulation of *FAB* genes exclusively depends on plastid-derived, GUN-mediated signals. The blue light receptor CRY1 and the TF HY5 were shown to be positive regulators of (abiotic stress-induced) anthocyanin biosynthesis [74,75,88,89] and knockout of both factors also led to anthocyanin deficiency after NF-treatment (figure 5 and Ruckle & Larkin [83]). Because anthocyanin content of *cry1-2* and *hy5* resembled that of *gun1 gun5*, it is reasonable to speculate that GUN-dependent signalling acts in concert with components of light signalling pathways to regulate FAB [31,83]. Indeed, the two *FAB* representatives *CHS* and *LDOX* were downregulated in *hy5* and to a stronger extent in *cry1-2* compared to WT, where the expression of these genes was comparable to that in *gun1* and *gun5*. On the other hand, while *CRY1* expression was slightly induced in *gun1* and *gun5* compared to the NF-treated WT, expression of *HY5*, which is induced in NF-treated WT (figure 1) and in a mutant with defects in plastid protein import [51], was reduced in *gun1* and *gun5* (figure 5; electronic supplementary material, table SI). Reduced expression of *HY5* correlated with modified expression of *FAB* genes in *gun* mutants. Furthermore, accelerated proteasomal degradation of HY5 in *cry1-2* [90,91] can, at least partially, explain the deregulation of *FAB* expression in the photoreceptor mutant. Although differently interpreted at that time, previous work already indicated that GUN1-dependent signalling requires CRY1 and HY5 for WT-like accumulation of anthocyanins when plastid development is blocked by lincomycin in blue light [83]. Therefore, a yet unknown connection of GUN1 and tetrapyrrole specific retrograde signals and the action of CRY1 and HY5 regulating the expression of *FAB* genes is proposed.

We cannot rule out that GUNs are also involved in a putative retrograde signalling cascade regulating *FAB* genes in high light (i.e. during operational control, Pogson *et al.* [1]), but our results rather suggest a correlation between the chlorophyll content and the ability to accumulate anthocyanins in various genotypes (electronic supplementary material, figure S2). While CRY1 and HY5 are essential, lack of

GUN1 did not interfere with the accumulation of anthocyanins when plants germinated in high light [83]. In conclusion, photosynthesis or a connected process might serve as a signal for or is involved in *FAB* induction under increased growth light intensities, which is in agreement with previous assumptions [55,78,79]. It is also not excluded that alteration of plastid tetrapyrrole biosynthesis interferes with light signalling pathways needed to perceive and integrate ultraviolet, blue or red light stimuli in order to induce anthocyanin biosynthesis.

(c) Connection of flavonoid/anthocyanin biosynthesis and *PHANG*

Although reduced expression of *PHANGs* correlated with a stimulated transcription of *FAB* genes in NF-treated WT (figure 1) and *gun* mutants show higher expression of *PHANGs* but reduced induction of *FAB* genes after NF treatment (figures 2 and 3), anthocyanins are probably not involved in the retrograde signalling-mediated control of *PHANG* expression. Firstly, lack of anthocyanins in FAB pathway mutants (figure 4) [92], as well as *cry1-2* and *hy5* (figure 5), did not prevent repression of *PHANGs* and, secondly, stronger accumulation of anthocyanins in the dominant *pap1-D* mutant resulted in WT-like repression of *PHANGs* when chloroplast development was perturbed (figure 4). In addition, even diminished accumulation of anthocyanins in *ref3-3 gun* double mutants compared to the single mutants, did not further uncouple *PHANG* expression from the developmental state of the plastids (figure 4). Thus, we propose that *PHANGs* and *FABs* are inversely co-regulated sets of nuclear-encoded genes whose regulation depends on GUN-proteins during biogenesis of plastids. The proposed co-regulation depends on TFs recognizing common regulatory motives in the promoter of their target genes. Indeed, promotor regions of classical targets of GUN-dependent signalling contain the G-box motif (CACGTA) needed for light-induced regulation of *PHANGs* [93,94]. Previous reports also revealed that *FAB* genes, including *CHS*, *DFR*, *LDOX* and *MYB75*, are controlled through TFs binding to G-Box and ACE elements. One of the most important TFs for light-dependent stimulation of gene products involved in FAB is HY5 binding to the regulatory elements [74,95–97] supporting our and the results of other studies (figure 5; Ruckle & Larkin [83]). HY5 has also been shown to act as a negative factor in GUN-dependent regulation of *PHANGs* when plastid development is arrested [31,98]. Based on the previous findings, the NF-induced expression in WT (figure 1) and reduced expression of *HY5* in *gun* mutants after NF-treatment (figure 5), the assumed co-regulation of *PHANGs* and *FABs* by a GUN signalling could be achieved through HY5.

In summary, our data reveal and emphasize the important function of GUN-dependent retrograde communication for the induction of *FAB* gene expression and accumulation of protective anthocyanin pigments during plastid biogenesis, one of the most sensitive processes in the course of plant development and establishment of photoautotrophy. Repression of *PHANGs* and induction of *FABs* through the same signalling pathway allows proper acclimation when plants suffer from adverse environmental conditions. Future research has to reveal how the import of plastid proteins (GUN1 specific), tetrapyrrole biosynthesis as well as known and unknown factors of light signalling cascades are connected to the regulation of secondary metabolism during plastid development.

4. Methods

(a) Plant material and growth conditions

Unless otherwise stated, *Arabidopsis* seeds (genotypes are listed in the electronic supplementary material, table SII) were surface-sterilized and plated on half-strength Murashige-Skoog (MS) medium (4.4 g l^{-1} MS medium, 0.5 g l^{-1} 2-(N-morpholino)ethanesulfonic acid, 1% agar, pH 5.7). After stratification for 2 days at 4°C, plates were exposed to continuous light (100 µmol photons m^{-2} s^{-1}) at 20–22°C. For etiolation experiments, plates were illuminated for 2 h immediately after stratification and then transferred to darkness. In each case, samples were harvested 5 days later. High light experiments were performed with soil-grown plants. After two weeks of growth at short day (10 h light) plants were transferred to continuous light for 2 days. Plants were then treated with high light (350 µmol photons m^{-2} s^{-1}) for the indicated time points. Mutation, the presence of T-DNA or knockout of genes in the mutants was confirmed with PCR-based methods using genomic DNA or cDNA and primers listed in the electronic supplementary material, table SIII.

(b) Treatments

All treatments of seedlings were carried out by diluting the appropriate compounds in the growth medium. NF was added (from a 5 mM stock solution in 100% acetone; Sigma-Aldrich) to a final concentration (f.c.) of 5 µM.

(c) RNA isolation, cDNA synthesis and quantitative real-time polymerase chain reaction analysis

For qPCR analysis at least four samples, each consisting of about 50 pooled seedlings, were harvested, frozen in liquid nitrogen and crushed in a steel-ball mill. Samples were stored at −80°C until further use. RNA was isolated from crushed plant material using the citric acid method [99]. Quality and quantity of RNA were checked on 1.2% TBE agarose gels. After DNaseI treatment (Thermo Scientific) aliquots of RNA (1–2 µg) were transcribed into cDNA using Moloney Murine Leukemia Virus (M-MuLV) reverse transcriptase (Thermo Scientific) and oligo dT(18) primer. All steps were performed essentially according to the manufacturer's protocol. qPCR analysis was carried out in a CFX96-C1000 96-well plate thermocycler (Bio-Rad) using SYBR green dye (Bio-Tool). The primers used are listed in the electronic supplementary material, table SIII. Calculation of gene expression was performed with the Bio-Rad CFX-Manager Software 1.6 using the ΔΔC(t)method [100] and *ACTIN2* as reference.

(d) RNA sequencing

RNA sequencing (RNA-seq) analyses were performed with total RNA from 5-day-old seedlings grown in the presence of 5 µM NF. RNA was extracted as described above. After DNase treatment, RNA was purified using phenol/chloroform/isoamyl alcohol precipitation protocol. After washing with 70% ethanol (v/v), RNA was dried and resuspended in RNase-free water. RNA-seq was performed by Novogene (China). mRNA was enriched using oligo(dT) beads. mRNA was fragmented randomly by adding fragmentation buffer, cDNA was then synthesized using the fragmented mRNA as template and random hexamer primers. After ligation and sequencing-adaptor ligation, the double-stranded cDNA library was subjected to size selection and PCR enrichment. Paired-end read libraries were sequenced on the Illumina Platform HiSeq4000. The RNA-seq experiment was performed once with three biological replicates, each consisting of a pool of about 50 seedlings.

(e) RNA sequencing data analysis

Base-calling was performed using bcl2fastq (v. 2.16.0.10). Differential expression analysis was carried out using a local installation of the GALAXY platform [101]. Sequenced reads were processed with Trimmomatic (v. 0.36.2) [102] to eliminate adapters and low-quality sequences. If at least one of the reads of a pair had a length of less than 15 bp after trimming, both reads were discarded. Remaining reads were mapped to the *Arabidopsis* genome (TAIR 10) using the TopHat2 (v. 2.1.1) gapped-read mapper [103]. After mapping, we used Cufflinks (v. 2.2.1.2) to assemble our transcriptome using the Araport11 transcriptome annotation as reference for each library independently. The assemblies were merged using Cuffmerge (v. 2.2.1.2). Differential expression analysis was performed using Cuffdiff (v. 2.2.1.5) [103]. Tools were run with default parameters, except that the maximum intron length was set to 3000 bp. Venn diagrams were constructed using the VENNY 2.1 web interface (http://bioinfogp.cnb.csic.es/tools/venny/). Heat maps were built using Perseus software [104]. Gene ontology term (GoT) enrichment analysis was performed with the GoTermFinder tool [105].

(f) Quantification of anthocyanins

Anthocyanins were quantified according to the method described previously [65]. Briefly, seedlings were harvested, frozen in liquid nitrogen and homogenized using a ball-mill. Then, the frozen powder was resuspended in 1 ml of extraction buffer (18% 1-propanol and 1% HCl in water) and incubated for at least 2 h at room temperature in darkness. After centrifugation for 15 min (maximum speed, 4°C) absorbance (A) of the supernatant at 537 nm, 650 nm and 750 nm were determined. Anthocyanin content was calculated using the following formula: (A537-A750)-0.25×(A650-A750)/g fresh weight or dry weight, respectively.

(g) Metabolite profiling

Profiling of anthocyanins and flavonoids was carried out exactly as described previously [106].

Data accessibility. RNA-seq data acquired during this study are publicly available from the NCBI Gene Expression Omnibus (https://www.ncbi.nlm.nih.gov/geo/) under the accession no. GSE104868.

Authors' contributions. A.S.R. conceived and designed the study, performed the experiments and wrote the article. T.T. performed mass spectrometric analysis. A.S.R., T.T., A.R.F. and B.G. revised the manuscript. All authors gave final approval for publication and agreed to be held accountable for the work performed therein.

Competing interests. The authors declare no competing interests.

Funding. The work was financed by a grant to B.G. (Subproject C04 of TRR 175 'The Green Hub', DFG, Germany) and to A.R.F. (subproject B04 of TRR 175 'The Green Hub', DFG, Germany). Work in the laboratory of A.S.R. is supported by a startup grant from the DFG funded TRR 175 'The Green Hub'.

Acknowledgements. We acknowledge the gifts of mutant seeds by Wout Boerjan and Ruben Vanholme (University Gent, Belgium), Steven J. Rothstein (University of Guelph, Canada), Clint Chapple (Purdue University, West Lafayette, Ind., USA) and Tatjana Kleine and Dario Leister (Ludwig-Maximilians-Universität Munich). We also thank José M. Muino (Humboldt University Berlin) for the support with the RNA-seq analysis and Leonardo Perez de Souza (Max Planck Institute for Molecular Plant Physiology, Potsdam-Golm) for supportive analysis of GC/LC-MS data.

References

1. Pogson BJ, Woo NS, Forster B, Small ID. 2008 Plastid signaling to the nucleus and beyond. *Trends Plant Sci.* **13**, 602–609. (doi:10.1016/j.tplants.2008.08.008)
2. Xiao Y *et al.* 2012 Retrograde signaling by the plastidial metabolite MEcPP regulates expression of nuclear stress-response genes. *Cell* **149**, 1525–1535. (doi:10.1016/j.cell.2012.04.038)
3. Benn G, Bjornson M, Ke H, De Souza A, Balmond EI, Shaw JT, Dehesh K. 2016 Plastidial metabolite MEcPP induces a transcriptionally centered stress-response hub via the transcription factor CAMTA3. *Proc. Natl Acad. Sci. USA* **113**, 8855–8860. (doi:10.1073/pnas.1602582113)
4. Jiang J *et al.* 2018 Interplay of the two ancient metabolites auxin and MEcPP regulates adaptive growth. *Nat. Commun.* **9**, 2262. (doi:10.1038/s41467-018-04708-5)
5. Estavillo GM *et al.* 2011 Evidence for a SAL1-PAP chloroplast retrograde pathway that functions in drought and high light signaling in *Arabidopsis*. *Plant Cell* **23**, 3992–4012. (doi:10.1105/tpc.111.091033)
6. Fang X, Zhao G, Zhang S, Li Y, Gu H, Li Y, Zhao Q, Qi Y. 2019 Chloroplast-to-nucleus signaling regulates MicroRNA biogenesis in *Arabidopsis*. *Dev. Cell* **48**, 371–382. (doi:10.1016/j.devcel.2018.11.046)
7. Woodson JD, Perez-Ruiz JM, Chory J. 2011 Heme synthesis by plastid ferrochelatase I regulates nuclear gene expression in plants. *Curr. Biol.* **21**, 897–903. (doi:10.1016/j.cub.2011.04.004)
8. Duanmu D *et al.* 2013 Retrograde bilin signaling enables *Chlamydomonas* greening and phototrophic survival. *Proc. Natl Acad. Sci. USA* **110**, 3621–3626. (doi:10.1073/pnas.1222375110)
9. Dietzel L *et al.* 2015 Identification of early nuclear target genes of plastidial redox signals that trigger the long-term response of *Arabidopsis* to light quality shifts. *Mol. Plant* **8**, 1237–1252. (doi:10.1016/j.molp.2015.03.004)
10. Dietz KJ, Turkan I, Krieger-Liszkay A. 2016 Redox- and reactive oxygen species-dependent signaling into and out of the photosynthesizing chloroplast. *Plant Physiol.* **171**, 1541–1550. (doi:10.1104/pp.16.00375)
11. Diaz MG, Hernandez-Verdeja T, Kremnev D, Crawford T, Dubreuil C, Strand A. 2018 Redox regulation of PEP activity during seedling establishment in *Arabidopsis thaliana*. *Nat. Commun.* **9**, 50. (doi:10.1038/s41467-017-02468-2)
12. Lee KP, Kim C, Landgraf F, Apel K. 2007 EXECUTER1- and EXECUTER2-dependent transfer of stress-related signals from the plastid to the nucleus of *Arabidopsis thaliana*. *Proc. Natl Acad. Sci. USA* **104**, 10 270–10 275. (doi:10.1073/pnas.0702061104)
13. Page MT, McCormac AC, Smith AG, Terry MJ. 2016 Singlet oxygen initiates a plastid signal controlling photosynthetic gene expression. *New Phytol.* **213**, 1168–1180. (doi:10.1111/nph.14223)
14. Kim C, Meskauskiene R, Zhang S, Lee KP, Lakshmanan Ashok M, Blajecka K, Herrfurth C, Feussner I, Apel K. 2012 Chloroplasts of *Arabidopsis* are the source and a primary target of a plant-specific programmed cell death signaling pathway. *Plant Cell* **24**, 3026–3039. (doi:10.1105/tpc.112.100479)
15. Exposito-Rodriguez M, Laissue PP, Yvon-Durocher G, Smirnoff N, Mullineaux P. M. 2017 Photosynthesis-dependent H_2O_2 transfer from chloroplasts to nuclei provides a high-light signaling mechanism. *Nat. Commun.* **8**, 49. (doi:10.1038/s41467-017-00074-w)
16. Willems P, Mhamdi A, Stael S, Storme V, Kerchev P, Noctor G, Gevaert K, Van Breusegem F. 2016 The ROS wheel: refining ROS transcriptional footprints. *Plant Physiol.* **171**, 1720–1733. (doi:10.1104/pp.16.00420)
17. Avendano-Vazquez AO *et al.* 2014 An uncharacterized apocarotenoid-derived signal generated in ζ-carotene desaturase mutants regulates leaf development and the expression of chloroplast and nuclear genes in *Arabidopsis*. *Plant Cell* **26**, 2524–2537. (doi:10.1105/tpc.114.123349)
18. Ramel F, Birtic S, Ginies C, Soubigou-Taconnat L, Triantaphylides C, Havaux M. 2012 Carotenoid oxidation products are stress signals that mediate gene responses to singlet oxygen in plants. *Proc. Natl Acad. Sci. USA* **109**, 5535–5540. (doi:10.1073/pnas.1115982109)

19. Grubler B *et al.* 2017 Light and plastid signals regulate different sets of genes in the albino mutant Pap7–1. *Plant Physiol.* **175**, 1203–1219. (doi:10.1104/pp.17.00982)
20. Kindgren P, Kremnev D, Blanco NE, de Dios Barajas Lopez J, Fernandez AP, Tellgren-Roth C, Kleine T, Small I, Strand A. 2012 The plastid redox insensitive 2 mutant of *Arabidopsis* is impaired in PEP activity and high light-dependent plastid redox signaling to the nucleus. *Plant J.* **70**, 279–291. (doi:10.1111/j.1365-313X.2011.04865.x)
21. Kleine T, Voigt C, Leister D. 2009 Plastid signaling to the nucleus: messengers still lost in the mists? *Trends Genet.* **25**, 185–192. (doi:10.1016/j.tig.2009.02.004)
22. Hernandez-Verdeja T, Strand A. 2018 Retrograde signals navigate the path to chloroplast development. *Plant Physiol.* **176**, 967–976. (doi:10.1104/pp.17.01299)
23. de Souza A, Wang JZ, Dehesh K. 2017 Retrograde signals: integrators of interorganellar communication and orchestrators of plant development. *Annu. Rev. Plant Biol.* **68**, 85–108. (doi:10.1146/annurev-arplant-042916-041007)
24. Chan KX, Phua SY, Crisp P, McQuinn R, Pogson BJ. 2015 Learning the languages of the chloroplast: retrograde signaling and beyond. *Annu. Rev. Plant Biol.* **67**, 25–53. (doi:10.1146/annurev-arplant-043015-111854)
25. Kleine T, Leister D. 2016 Retrograde signaling: organelles go networking. *Biochim. Biophys. Acta* **1857**, 1313–1325. (doi:10.1016/j.bbabio.2016.03.017)
26. Petrillo E *et al.* 2014 A chloroplast retrograde signal regulates nuclear alternative splicing. *Science* **344**, 427–430. (doi:10.1126/science.1250322)
27. Woodson JD, Joens MS, Sinson AB, Gilkerson J, Salome PA, Weigel D, Fitzpatrick JA, Chory J. 2015 Ubiquitin facilitates a quality-control pathway that removes damaged chloroplasts. *Science* **350**, 450–454. (doi:10.1126/science.aac7444)
28. Ortiz-Alcaide M, Llamas E, Gomez-Cadenas A, Nagatani A, Martinez-Garcia J. F, Rodriguez-Concepcion M. 2019 Chloroplasts modulate elongation responses to canopy shade by retrograde pathways involving hy5 and abscisic acid. *Plant Cell* **31**, 384–398. (doi:10.1105/tpc.18.00617)
29. Hess WR, Muller A, Nagy F, Borner T. 1994 Ribosome-deficient plastids affect transcription of light-induced nuclear genes: genetic evidence for a plastid-derived signal. *Mol. Gen. Genet.* **242**, 305–312. (doi:10.1007/BF00280420)
30. Susek RE, Ausubel FM, Chory J. 1993 Signal transduction mutants of *Arabidopsis* uncouple nuclear CAB and RBCS gene expression from chloroplast development. *Cell* **74**, 787–799. (doi:10.1016/0092-8674(93)90459-4)
31. Ruckle ME, DeMarco SM, Larkin RM. 2007 Plastid signals remodel light signaling networks and are essential for efficient chloroplast biogenesis in *Arabidopsis*. *Plant Cell* **19**, 3944–3960. (doi:10.1105/tpc.107.054312)
32. Zhao X, Huang J, Chory J. 2019 GUN1 interacts with MORF2 to regulate plastid RNA editing during retrograde signaling. *Proc. Natl Acad. Sci. USA* **116**, 201820426. (doi:10.1073/pnas.1820426116)
33. Wu GZ, Meyer EH, Wu S, Bock R. 2019 Extensive post-transcriptional regulation of nuclear gene expression by plastid retrograde signals. *Plant Physiol.* **180**, 421. (doi:10.1104/pp.19.00421)
34. Wu GZ *et al.* 2019 Control of retrograde signaling by protein import and cytosolic folding stress. *Nat Plants* **5**, 525–538. (doi:10.1038/s41477-019-0415-y)
35. Woodson JD, Perez-Ruiz JM, Schmitz RJ, Ecker JR, Chory J. 2012 Sigma factor-mediated plastid retrograde signals control nuclear gene expression. *Plant J.* **73**, 1–13. (doi:10.1111/tpj.12011)
36. Voigt C, Oster U, Bornke F, Jahns P, Dietz KJ, Leister D, Kleine T. 2010 In-depth analysis of the distinctive effects of norflurazon implies that tetrapyrrole biosynthesis, organellar gene expression and ABA cooperate in the GUN-type of plastid signaling. *Physiol. Plant.* **138**, 503–519. (doi:10.1111/j.1399-3054.2009.01343.x)
37. Terry MJ, Smith AG. 2013 A model for tetrapyrrole synthesis as the primary mechanism for plastid-to-nucleus signaling during chloroplast biogenesis. *Front. Plant Sci.* **4**, 14. (doi:10.3389/fpls.2013.00014)
38. Tadini L *et al.* 2016 GUN1 controls accumulation of the plastid ribosomal protein S1 at the protein level and interacts with proteins involved in plastid protein homeostasis. *Plant Physiol.* **170**, 1817–1830. (doi:10.1104/pp.15.02033)
39. Pesaresi P, Kim C. 2019 Current understanding of GUN1: a key mediator involved in biogenic retrograde signaling. *Plant Cell Rep.* **38**, 819–823. (doi:10.1007/s00299-019-02383-4)
40. Marino G, Naranjo B, Wang J, Penzler JF, Kleine T, Leister D. 2019 Relationship of GUN1 to FUG1 in chloroplast protein homeostasis. *Plant J.* **99**, 521–555. (doi:10.1111/tpj.14342)
41. Cottage A, Mott EK, Kempster JA, Gray J. C. 2010 The *Arabidopsis* plastid-signaling mutant gun1 (genomes uncoupled1) shows altered sensitivity to sucrose and abscisic acid and alterations in early seedling development. *J. Exp. Bot.* **61**, 3773–3786. (doi:10.1093/jxb/erq186)
42. Colombo M, Tadini L, Peracchio C, Ferrari R, Pesaresi P. 2016 GUN1, a jack-of-all-trades in chloroplast protein homeostasis and signaling. *Front. Plant Sci.* **7**, 1427. (doi:10.3389/fpls.2016.01427)
43. Peter E, Grimm B. 2009 GUN4 is required for posttranslational control of plant tetrapyrrole biosynthesis. *Mol. Plant* **2**, 1198–1210. (doi:10.1093/mp/ssp072)
44. Larkin RM, Alonso JM, Ecker JR, Chory J. 2003 GUN4, a regulator of chlorophyll synthesis and intracellular signaling. *Science* **299**, 902–906. (doi:10.1126/science.1079978)
45. Huang YS, Li HM. 2009 *Arabidopsis* CHLI2 can substitute for CHLI1. *Plant Physiol.* **150**, 636–645. (doi:10.1104/pp.109.135368)
46. Gadjieva R, Axelsson E, Olsson U, Hansson M. 2005 Analysis of gun phenotype in barley magnesium chelatase and Mg-protoporphyrin IX monomethyl ester cyclase mutants. *Plant Physiol. Biochem.* **43**, 901–908. (doi:10.1016/j.plaphy.2005.08.003)
47. Mochizuki N, Tanaka R, Tanaka A, Masuda T, Nagatani A. 2008 The steady-state level of Mg-protoporphyrin IX is not a determinant of plastid-to-nucleus signaling in *Arabidopsis*. *Proc. Natl Acad. Sci. USA* **105**, 15 184–15 189. (doi:10.1073/pnas.0803245105)
48. Moulin M, McCormac AC, Terry MJ, Smith AG. 2008 Tetrapyrrole profiling in *Arabidopsis* seedlings reveals that retrograde plastid nuclear signaling is not due to Mg-protoporphyrin IX accumulation. *Proc. Natl Acad. Sci. USA* **105**, 15 178–15 183. (doi:10.1073/pnas.0803054105)
49. Larkin R. M. 2016 Tetrapyrrole signaling in plants. *Front. Plant Sci.* **7**, 1586. (doi:10.3389/fpls.2016.01586)
50. Leister D, Kleine T. 2016 Definition of a core module for the nuclear retrograde response to altered organellar gene expression identifies GLK overexpressors as gun mutants. *Physiol. Plant.* **157**, 297–309. (doi:10.1111/ppl.12431)
51. Kakizaki T, Matsumura H, Nakayama K, Che FS, Terauchi R, Inaba T. 2009 Coordination of plastid protein import and nuclear gene expression by plastid-to-nucleus retrograde signaling. *Plant Physiol.* **151**, 1339–1353. (doi:10.1104/pp.109.145987)
52. Kacprzak SM, Mochizuki N, Naranjo B, Xu D, Leister D, Kleine T, Okamoto H, Terry MJ. 2019 Plastid-to-nucleus retrograde signaling during chloroplast biogenesis does not require ABI4. *Plant Physiol.* **179**, 18–23. (doi:10.1104/pp.18.01047)
53. Gould KS, Jay-Allemand C, Logan BA, Baissac Y, Bidel LPR. 2018 When are foliar anthocyanins useful to plants? Re-evaluation of the photoprotection hypothesis using *Arabidopsis thaliana* mutants that differ in anthocyanin accumulation. *Environ. Exp. Bot.* **154**, 11–22. (doi:10.1016/j.envexpbot.2018.02.006)
54. Gould KS. 2004 Nature's Swiss army knife: the diverse protective roles of anthocyanins in leaves. *J. Biomed. Biotechnol.* **2004**, 314–320. (doi:10.1155/S1110724304406147)
55. Xu Z, Mahmood K, Rothstein SJ. 2017 ROS Induces anthocyanin production via late biosynthetic genes and anthocyanin deficiency confers the hypersensitivity to ROS-generating stresses in *Arabidopsis*. *Plant Cell Physiol.* **58**, 1364–1377. (doi:10.1093/pcp/pcx073)
56. Vogt T. 2010 Phenylpropanoid biosynthesis. *Mol. Plant* **3**, 2–20. (doi:10.1093/mp/ssp106)
57. Fraser CM, Chapple C. 2011 The phenylpropanoid pathway in *Arabidopsis*. *Arabidopsis Book/Am. Soc. Plant Biol.* **9**, e0152. (doi:10.1199/tab.0152)
58. Appelhagen I, Thiedig K, Nordholt N, Schmidt N, Huep G, Sagasser M, Weisshaar B. 2014 Update on transparent testa mutants from *Arabidopsis thaliana*: characterisation of new alleles from an

isogenic collection. *Planta* **240**, 955–970. (doi:10.1007/s00425-014-2088-0)

59. Passeri V, Koes R, Quattrocchio F. M. 2016 New challenges for the design of high value plant products: stabilization of anthocyanins in plant vacuoles. *Front. Plant Sci.* **7**, 153. (doi:10.3389/fpls.2016.00153)
60. Jaakola L. 2013 New insights into the regulation of anthocyanin biosynthesis in fruits. *Trends Plant Sci.* **18**, 477–483. (doi:10.1016/j.tplants.2013.06.003)
61. Maier A *et al.* 2013 Light and the E3 ubiquitin ligase COP1/SPA control the protein stability of the MYB transcription factors PAP1 and PAP2 involved in anthocyanin accumulation in *Arabidopsis*. *Plant J.* **74**, 638–651. (doi:10.1111/tpj.12153)
62. Zhang X, Abrahan C, Colquhoun T. A, Liu C. J. 2017 A proteolytic regulator controlling chalcone synthase stability and flavonoid biosynthesis in *Arabidopsis*. *Plant Cell* **29**, 1157–1174. (doi:10.1105/tpc.16.00855)
63. Zhang X, Gou M, Liu CJ. 2013 *Arabidopsis* Kelch repeat F-box proteins regulate phenylpropanoid biosynthesis via controlling the turnover of phenylalanine ammonia-lyase. *Plant Cell* **25**, 4994–5010. (doi:10.1105/tpc.113.119644)
64. Stracke R, Ishihara H, Huep G, Barsch A, Mehrtens F, Niehaus K, Weisshaar B. 2007 Differential regulation of closely related R2R3-MYB transcription factors controls flavonol accumulation in different parts of the *Arabidopsis thaliana* seedling. *Plant J.* **50**, 660–677. (doi:10.1111/j.1365-313X.2007.03078.x)
65. Lotkowska ME, Tohge T, Fernie AR, Xue GP, Balazadeh S, Mueller-Roeber B. 2015 The *Arabidopsis* transcription factor MYB112 promotes anthocyanin formation during salinity and under high light stress. *Plant Physiol.* **169**, 1862–1880. (doi:10.1104/pp.15.00605)
66. Shi MZ, Xie DY. 2014 Biosynthesis and metabolic engineering of anthocyanins in *Arabidopsis thaliana*. *Recent Pat. Biotechnol.* **8**, 47–60. (doi:10.2174/1872208307666131218123538)
67. Lloyd A, Brockman A, Aguirre L, Campbell A, Bean A, Cantero A, Gonzalez A. 2017 Advances in the MYB-bHLH-WD Repeat (MBW) pigment regulatory model: addition of a wrky factor and co-option of an anthocyanin myb for betalain regulation. *Plant Cell Physiol.* **58**, 1431–1441. (doi:10.1093/pcp/pcx075)
68. Zhang F, Gonzalez A, Zhao M, Payne C. T, Lloyd A. 2003 A network of redundant bHLH proteins functions in all TTG1-dependent pathways of *Arabidopsis*. *Development* **130**, 4859–4869. (doi:10.1242/dev.00681)
69. Dubos C *et al.* 2008 MYBL2 is a new regulator of flavonoid biosynthesis in *Arabidopsis thaliana*. *Plant J.* **55**, 940–953. (doi:10.1111/j.1365-313X.2008.03564.x)
70. Nguyen NH, Jeong CY, Kang GH, Yoo SD, Hong S. W, Lee H. 2015 MYBD employed by HY5 increases anthocyanin accumulation via repression of MYBL2 in *Arabidopsis*. *Plant J.* **84**, 1192–1205. (doi:10.1111/tpj.13077)
71. Wang Y, Wang Y, Song Z, Zhang H. 2016 Repression of MYBL2 by both microRNA858a and HY5 leads to the activation of anthocyanin biosynthetic pathway in *Arabidopsis*. *Mol. Plant* **9**, 1395–1405. (doi:10.1016/j.molp.2016.07.003)
72. Xie Y, Tan H, Ma Z, Huang J. 2016 DELLA proteins promote anthocyanin biosynthesis via sequestering MYBL2 and JAZ suppressors of the MYB/bHLH/WD40 complex in *Arabidopsis thaliana*. *Mol. Plant* **9**, 711–721. (doi:10.1016/j.molp.2016.01.014)
73. Stracke R, Favory JJ, Gruber H, Bartelniewoehner L, Bartels S, Binkert M, Funk M, Weisshaar B, Ulm R. 2010 The *Arabidopsis* bZIP transcription factor HY5 regulates expression of the PFG1/MYB12 gene in response to light and ultraviolet-B radiation. *Plant Cell Environ.* **33**, 88–103. (doi:10.1111/j.1365-3040.2009.02061.x)
74. Shin DH, Choi M, Kim K, Bang G, Cho M, Choi SB, Choi G, Park YI. 2013 HY5 regulates anthocyanin biosynthesis by inducing the transcriptional activation of the MYB75/PAP1 transcription factor in *Arabidopsis*. *FEBS Lett.* **587**, 1543–1547. (doi:10.1016/j.febslet.2013.03.037)
75. Gao J, Wang X, Zhang M, Bian M, Deng W, Zuo Z, Yang Z, Zhong D, Lin C. 2015 Trp triad-dependent rapid photoreduction is not required for the function of *Arabidopsis* CRY1. *Proc. Natl Acad. Sci. USA* **112**, 9135–9140. (doi:10.1073/pnas.1504404112)
76. Warnasooriya SN, Porter KJ, Montgomery BL. 2011 Tissue- and isoform-specific phytochrome regulation of light-dependent anthocyanin accumulation in *Arabidopsis thaliana*. *Plant Signal Behav.* **6**, 624–631. (doi:10.4161/psb.6.5.15084)
77. Heijde M *et al.* 2013 Constitutively active UVR8 photoreceptor variant in *Arabidopsis*. *Proc. Natl Acad. Sci. USA* **110**, 20 326–20 331. (doi:10.1073/pnas.1314336110)
78. Das PK, Shin DH, Choi SB, Yoo SD, Choi G, Park YI. 2012 Cytokinins enhance sugar-induced anthocyanin biosynthesis in *Arabidopsis*. *Mol. Cells* **34**, 93–101. (doi:10.1007/s10059-012-0114-2)
79. Das PK, Geul B, Choi SB, Yoo S. D, Park Y. I. 2011 Photosynthesis-dependent anthocyanin pigmentation in *Arabidopsis*. *Plant Signal Behav.* **6**, 23–25. (doi:10.4161/psb.6.1.14082)
80. Qi T *et al.* 2011 The Jasmonate-ZIM-domain proteins interact with the WD-Repeat/bHLH/MYB complexes to regulate Jasmonate-mediated anthocyanin accumulation and trichome initiation in *Arabidopsis thaliana*. *Plant Cell* **23**, 1795–1814. (doi:10.1105/tpc.111.083261)
81. Nott A, Jung HS, Koussevitzky S, Chory J. 2006 Plastid-to-nucleus retrograde signaling. *Annu. Rev. Plant Biol.* **57**, 739–759. (doi:10.1146/annurev.arplant.57.032905.105310)
82. Kovinich N, Kayanja G, Chanoca A, Otegui M. S, Grotewold E. 2015 Abiotic stresses induce different localizations of anthocyanins in *Arabidopsis*. *Plant Signal Behav.* **10**, e1027850. (doi:10.1080/15592324.2015.1027850)
83. Ruckle ME, Larkin RM. 2009 Plastid signals that affect photomorphogenesis in *Arabidopsis thaliana* are dependent on GENOMES UNCOUPLED 1 and cryptochrome 1. *New Phytol.* **182**, 367–379. (doi:10.1111/j.1469-8137.2008.02729.x)
84. Kim S, Hwang G, Lee S, Zhu JY, Paik I, Nguyen TT, Kim J, Oh E. 2017 High ambient temperature represses anthocyanin biosynthesis through degradation of HY5. *Front. Plant Sci.* **8**, 1787. (doi:10.3389/fpls.2017.01787)
85. Oelmuller R, Levitan I, Bergfeld R, Rajasekhar V. K, Mohr H. 1986 Expression of nuclear genes as affected by treatments acting on the plastids. *Planta* **168**, 482–492. (doi:10.1007/Bf00392267)
86. Saini G, Meskauskiene R, Pijacka W, Roszak P, Sjogren LL, Clarke AK, Straus M, Apel K. 2011 'happy on norflurazon' (hon) mutations implicate perturbance of plastid homeostasis with activating stress acclimatization and changing nuclear gene expression in norflurazon-treated seedlings. *Plant J.* **65**, 690–702. (doi:10.1111/j.1365-313X.2010.04454.x)
87. Mochizuki N, Brusslan JA, Larkin R, Nagatani A, Chory J. 2001 *Arabidopsis* genomes uncoupled 5 (GUN5) mutant reveals the involvement of Mg-chelatase H subunit in plastid-to-nucleus signal transduction. *Proc. Natl Acad. Sci USA* **98**, 2053–2058. (doi:10.1073/pnas.98.4.2053)
88. Zhang Y, Zheng S, Liu Z, Wang L, Bi Y. 2011 Both HY5 and HYH are necessary regulators for low temperature-induced anthocyanin accumulation in *Arabidopsis* seedlings. *J. Plant Physiol.* **168**, 367–374. (doi:10.1016/j.jplph.2010.07.025)
89. Liu CC, Chi C, Jin LJ, Zhu J, Yu J. Q, Zhou Y. H. 2018 The bZip transcription factor HY5 mediates CRY1a-induced anthocyanin biosynthesis in tomato. *Plant Cell Environ.* **41**, 1762–1775. (doi:10.1111/pce.13171)
90. Osterlund MT, Hardtke CS, Wei N, Deng X. W. 2000 Targeted destabilization of HY5 during light-regulated development of *Arabidopsis*. *Nature* **405**, 462–466. (doi:10.1038/35013076)
91. Jia KP, Luo Q, He SB, Lu XD, Yang HQ. 2014 Strigolactone-regulated hypocotyl elongation is dependent on cryptochrome and phytochrome signaling pathways in *Arabidopsis*. *Mol. Plant* **7**, 528–540. (doi:10.1093/mp/sst093)
92. Xu D, Dhiman R, Garibay A, Mock H-P, Leister D, Kleine T. 2020 Cellulose defects in the *Arabidopsis* secondary cell wall promote early chloroplast development. *plantJ.* **101**, 156–170.
93. Strand A, Asami T, Alonso J, Ecker JR, Chory J. 2003 Chloroplast to nucleus communication triggered by accumulation of Mg-protoporphyrinIX. *Nature* **421**, 79–83. (doi:10.1038/nature01204)
94. Chattopadhyay S, Ang LH, Puente P, Deng XW, Wei N. 1998 *Arabidopsis* bZIP protein HY5 directly interacts with light-responsive promoters in mediating light control of gene expression. *Plant Cell* **10**, 673–683. (doi:10.1105/tpc.10.5.673)
95. Kleine T, Kindgren P, Benedict C, Hendrickson L, Strand A. 2007 Genome-wide gene expression analysis reveals a critical role for CRYPTOCHROME1 in the response of *Arabidopsis* to high irradiance.

Plant Physiol. **144**, 1391–1406. (doi:10.1104/pp.107.098293)

96. Gangappa S. N, Botto J. F. 2016 The multifaceted roles of HY5 in plant growth and development. *Mol. Plant* **9**, 1353–1365. (doi:10.1016/j.molp.2016.07.002)
97. Dao TT, Linthorst HJ, Verpoorte R. 2011 Chalcone synthase and its functions in plant resistance. *Phytochem. Rev.* **10**, 397–412. (doi:10.1007/s11101-011-9211-7)
98. Kindgren P, Noren L, Lopez Jde D, Shaikhali J, Strand A. 2012 Interplay between Heat Shock Protein 90 and HY5 controls PhANG expression in response to the GUN5 plastid signal. *Mol. Plant* **5**, 901–913. (doi:10.1093/mp/ssr112)
99. Oñate-Sánchez L, Vicente-Carbajosa J. 2008 DNA-free RNA isolation protocols for *Arabidopsis thaliana*, including seeds and siliques. *BMC Res. Notes* **1**, 93. (doi:10.1186/1756-0500-1-93)
100. Pfaffl M. W. 2001 A new mathematical model for relative quantification in real-time RT-PCR. *Nucleic Acids Res.* **29**, e45. (doi:10.1093/nar/29.9.e45)
101. Gruning BA *et al.* 2017 The RNA workbench: best practices for RNA and high-throughput sequencing bioinformatics in Galaxy. *Nucleic Acids Res.* **45**, W560–W566. (doi:10.1093/nar/gkx409)
102. Bolger AM, Lohse M, Usadel B. 2014 Trimmomatic: a flexible trimmer for Illumina sequence data. *Bioinformatics* **30**, 2114–2120. (doi:10.1093/bioinformatics/btu170)
103. Trapnell C *et al.* 2012 Differential gene and transcript expression analysis of RNA-seq experiments with TopHat and Cufflinks. *Nat. Protoc.* **7**, 562–578. (doi:10.1038/nprot.2012.016)
104. Tyanova S, Temu T, Sinitcyn P, Carlson A, Hein MY, Geiger T, Mann M, Cox J. 2016 The Perseus computational platform for comprehensive analysis of (prote)omics data. *Nat. Methods* **13**, 731–740. (doi:10.1038/nmeth.3901)
105. Boyle EI, Weng S, Gollub J, Jin H, Botstein D, Cherry JM, Sherlock G. 2004 GO::TermFinder–open source software for accessing gene ontology information and finding significantly enriched gene ontology terms associated with a list of genes. *Bioinformatics* **20**, 3710–3715. (doi:10.1093/bioinformatics/bth456)
106. Alseekh S *et al.* 2015 Identification and mode of inheritance of quantitative trait loci for secondary metabolite abundance in tomato. *Plant Cell* **27**, 485–512. (doi:10.1105/tpc.114.132266)